

Damage Assessment of Adjacent Buildings with Fixed Bases under Earthquake Loads



Abbas Moustafa

Department of Civil Engineering,
Faculty of Engineering, Minia University,
Minia 61111, Egypt.
abbas.moustafa@yahoo.com

Sayed Mahmoud

Department of Civil Engineering,
Faculty of Engineering at Rabigh,
King Abdulaziz University, Saudi Arabia
elseedy@hotmail.com

SUMMARY:

This paper deals with damage assessment of adjacent insufficiently separated buildings under earthquake loads. In previous studies, the structure input-response pair is used to examine pounding effects on adjacent buildings. In this paper, pounding of adjacent buildings is assessed using input energy, dissipated energy and damage indices. These measures are calculated using nonlinear time-history analysis and provide quantitative estimates of structural damage and necessary repair. Adjacent buildings with flexible and stiff parameters are considered. The nonlinear viscoelastic model is used for capturing the induced pounding forces. Influences of the separation distance between buildings and yield characteristics on damage of adjacent buildings are investigated. Three input ground motions at near-fault and far-fault regions with different peak ground accelerations and soil condition are used in the analysis. Numerical illustrations on damage of fixed-base adjacent buildings are provided. The numerical results imply that the colliding force between adjacent buildings influences damage of both buildings.

Keywords: adjacent buildings, damage index, ductility, earthquake loads, inelastic structures

1. INTRODUCTION

The unexpected severe damage of infrastructures and buildings and the loss of lives during recent earthquakes, such as, the 12 January 2010 Haiti earthquake and the 11 March 2011 Tohoku Japan earthquake have raised significant questions and concerns within the earthquake engineering community. The earthquake resistance design of structures is the weapon against seismic loads [1]. In heavily populated regions and Mega cities, such as Cairo, buildings are constructed side to side without separation distances. This could cause coupling effects in adjacent structures under earthquake and wind loads. Mathematically, a coupling force appears in the equations of motion of both structures. A significant attention to this phenomenon has been paid after the 19 September 1985 Mexico earthquake in which about 40% of the collapsed or severely damaged buildings have experienced some level of pounding and in 15% of them pounding led to total collapse [2]. Pounding of adjacent structures has been extensively studied during the last two decades or so. Comprehensive reviews of literature on this subject can be found in Refs. [3-5]. Pounding occurs to adjacent structures due to the difference of their dynamic properties and the insufficient separation distance.

Nonlinear response of adjacent buildings has been studied by Athanassiadou and Penelis [6]. Anagnostopoulos [3] presented a comprehensive study on pounding of adjacent buildings modelled as SDOF nonlinear systems. Pantelides and Ma [7] considered the coupling behaviour of damped SDOF elastic and inelastic structures with one-sided pounding during earthquakes using the Hertz contact model. Muthukumar and Des Roches [8] studied pounding of adjacent structures modelled as elastic and inelastic SDOF systems using different pounding models. Jankowski [9] proposed the notion of the impact force response spectrum for elastic and inelastic adjacent structures. Pounding of structures modelled as MDOF systems has also been investigated in several studies (see, e.g., [10]).

In general, the coupling effect of adjacent buildings under earthquake loads is investigated by comparing the input ground motion and the associated structural response. This paper investigates damage of adjacent buildings with fixed-base. Damage of inelastic buildings is quantified in terms of damage indices and hysteretic energy dissipated by inelastic deformations. The next section provides a brief overview on damage quantification in structures under earthquake loads using damage indices. Section 3 demonstrates buildings and pounding models of adjacent inelastic buildings with fixed-base. Section 4 describes the system parameters for fixed-base buildings. A set of three strong ground motions used as input to adjacent structures and the response quantities are defined in the same section. Section 5 provides numerical illustrations on the formulation developed in this paper. Section 6 presents the main conclusions drawn based on the numerical results achieved in this study.

2. DAMAGE OF STRUCTURES UNDER EARTHQUAKE LOADS

A vast research has been carried out on damage of structures under strong ground motion. Moustafa [11] provided a comprehensive review on the literature of this subject. Damage indices can be estimated by comparing the response parameters demanded by the earthquake with the structural capacities. Powell and Allahabadi [12] proposed a damage index in terms of the ultimate ductility (capacity) μ_u and the maximum ductility (demand) attained during ground shaking μ_{\max} :

$$DI_{AP} = \frac{x_{\max} - x_y}{x_u - x_y} = \frac{\mu_{\max} - 1}{\mu_u - 1} \quad (2.1)$$

However DI_{AP} does not include effects from hysteretic energy dissipation. Fajfar [13] and Cosenza et al., [14] proposed a damage index based on the structure hysteretic energy E_H , given as:

$$DI_{FC} = \frac{E_H / (f_y x_y)}{\mu_u - 1} \quad (2.2)$$

where f_y, x_y, E_H are the yield strength, yield displacement, and hysteretic energy, respectively. A robust damage measure should include not only the maximum response but the effect of repeated cyclic loading as well. Park and co-workers developed a simple damage index, given as [15-17]:

$$DI_{PA} = \frac{x_{\max}}{x_u} + \gamma \frac{E_H}{f_y x_u} = \frac{\mu_{\max}}{\mu_u} + \gamma \frac{E_H}{f_y x_y \mu_u} \quad (2.3)$$

Here, x_{\max}, E_H are the maximum displacement and dissipated hysteretic energy (excluding elastic energy) under the earthquake. Note that x_{\max} is the maximum absolute value of the displacement response under the ground motion. x_u is the ultimate deformation capacity under monotonic loading and γ is a positive constant that weights the effect of cyclic loading on structural damage. Note that $\gamma = 0$ implies that the contribution to DI_{PA} from cyclic loading is omitted.

The state of the structure damage is defined as: (a) repairable damage, when $DI_{PA} < 0.40$, (b) damaged beyond repair, when $0.40 \leq DI_{PA} < 1.0$, and (c) total or complete collapse, when $DI_{PA} \geq 1.0$. These criteria are based on calibration of DI_{PA} against experimental results and field observations in earthquakes [17]. The Park and Ang damage index reveals that both maximum ductility and hysteretic energy dissipation contribute to the structure resistance during ground motions. In Eqn. 2.3, damage is expressed as a linear combination of the damage caused by excessive deformation and that contributed by repeated cyclic loading effect. Note also that the quantities x_{\max}, E_H depend on the loading history while the quantities γ, x_u, f_y are independent of the loading history and are determined from experimental tests.

Another measure of structural performance is given as the dissipated hysteretic energy normalized to the input energy to the structure. Mathematically, this index is given as:

$$DI_H = \frac{E_H}{E_I} \quad (2.4)$$

The quantification of the energy terms E_H and E_I is provided in Section 4.3. Note that the damage index of Eqn. 2.4 includes the structure's response demanded by the ground motion and the associated structural capacity parameters in an implicit form. Note also that DI_H close to zero implies a linear behavior while DI_H larger than zero indicates inelastic behavior and occurrence of structural damage

3. BUILDINGS AND POUNDING MODELS

In the present study, idealized mathematical models for adjacent SDOF fixed-base buildings situated at a gap distance d are considered. To numerically model the pounding phenomenon, a nonlinear spring in conjunction with a nonlinear dashpot element is used for estimating the induced pounding forces acting on the colliding masses.

3.1. Nonlinear buildings model

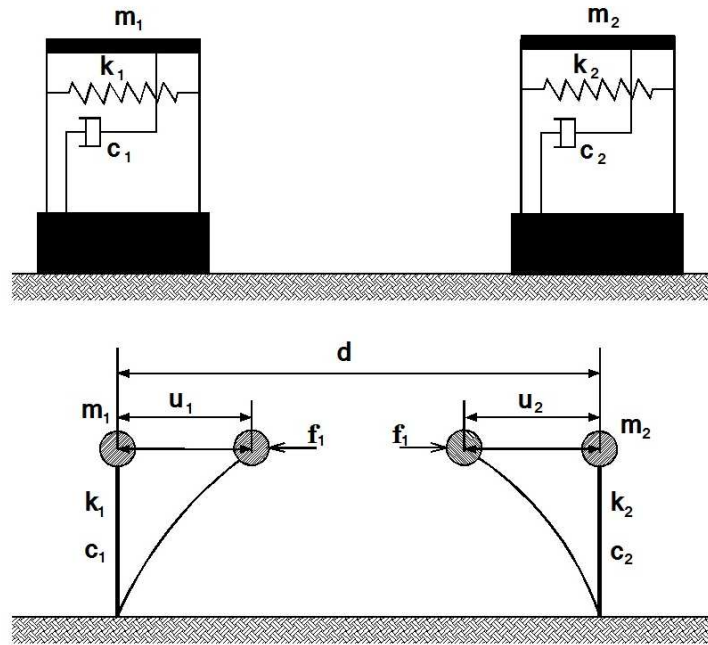


Figure 3.1. Colliding model for buildings with fixed bases

To assess damage of neighbouring buildings insufficiently separated, to allow occurrence of impact, buildings have been idealized as their masses lumped at the floor level, which are considered as rigid in their own plane, assuming that the superstructures to behave in an inelastic way during earthquake excitations. Let m_1 , c_1 , u_1 , r_1 and m_2 , c_2 , u_2 , r_2 be the masses, damping coefficients, displacements and restoring forces for the left and the right buildings, respectively. In the case of two structures with fixed bases (see Fig. 1), the nonlinear dynamic equation of motion can be written as:

$$\begin{pmatrix} m_1 & 0 \\ 0 & m_2 \end{pmatrix} \begin{pmatrix} \ddot{u}_1 \\ \ddot{u}_2 \end{pmatrix} + \begin{pmatrix} c_1 & 0 \\ 0 & c_2 \end{pmatrix} \begin{pmatrix} \dot{u}_1 \\ \dot{u}_2 \end{pmatrix} + \begin{pmatrix} r_1 \\ r_2 \end{pmatrix} + \begin{pmatrix} f_1 \\ -f_1 \end{pmatrix} = - \begin{pmatrix} m_1 & 0 \\ 0 & m_2 \end{pmatrix} \begin{pmatrix} \ddot{u}_g \\ \ddot{u}_g \end{pmatrix}, \quad (3.1)$$

where, \dot{u}_1 , \ddot{u}_1 and \dot{u}_2 , \ddot{u}_2 denote the velocities and accelerations of the left and the right structures, respectively; f_1 is the force due to impact (pounding force); and \ddot{u}_g is the earthquake acceleration.

During the elastic stage, the resisting forces, r_1 , r_2 , take the form: $r_1 = k_1 u_1$, $r_2 = k_2 u_2$, while during the plastic stage: r_1 varies between f_{y1} and $-f_{y1}$, and r_2 varies between f_{y2} and $-f_{y2}$, where k_1 , k_2 and f_{y1} , f_{y2} are the initial stiffness coefficients and yield strength for the left and the right buildings, respectively.

Assuming viscous damping model for both buildings, the values of initial natural period T_i and the damping coefficient c_i ($i=1, 2$) of the undamaged buildings are given as in[18]:

$$T_i = \frac{2\pi}{\omega_i}; \quad c_i = 2\xi_i \sqrt{k_i m_i} \quad (3.2)$$

Note that $\omega_i = \sqrt{\frac{k_i}{m_i}}$ is the natural frequency of the undamaged structure. The structural response of both buildings is estimated by solving the coupled differential Eqn. 3.1 numerically using the Newmark-Beta method.

3.2. Nonlinear pounding model

Pounding between adjacent structures is a highly complex phenomenon. Therefore, in order to accurately simulate impact, an appropriate impact force model must be adopted. The nonlinear viscoelastic model [19] which uses the general trend of the nonlinear Hertz law of contact together with an incorporated hysteretic damping function simulating the dissipation of energy during impact is utilized to capture impacting force. According to the nonlinear viscoelastic model, the pounding force between two adjacent buildings is given as [19]:

$$\begin{aligned} f_1 &= 0 & \text{for } \delta \leq 0 & \quad (\text{no contact}) \\ f_1 &= \bar{\beta} \delta^{\frac{3}{2}} + \bar{c} \dot{\delta} & \text{for } \delta > 0 \text{ and } \dot{\delta}(t) > 0 & \quad (\text{contact - approach period}) \\ f_1 &= \bar{\beta} \delta^{\frac{3}{2}} & \text{for } \delta > 0 \text{ and } \dot{\delta}(t) \leq 0 & \quad (\text{contact - restitution period}) \end{aligned} \quad (3.3)$$

Herein, $\delta = (u_1 - u_2 - d)$ is the relative displacement (d denotes the initial separation gap), $\bar{\beta}$ is the impact stiffness parameter and

$$\bar{c} = 2\bar{\xi} \sqrt{\bar{\beta} \sqrt{\delta} \frac{m_1 m_2}{m_1 + m_2}} \quad (3.4)$$

is the impact element's damping. Here, $\bar{\xi}$ is an impact damping ratio related to a coefficient of restitution, e , which can be defined as [20]:

$$\bar{\xi} = \frac{9\sqrt{5}}{2} \frac{1 - e^2}{e(e(9\pi - 16) + 16)} \quad (3.5)$$

4. SYSTEM PARAMETERS AND INPUT GROUND MOTIONS

This section defines the parameters of adjacent buildings as well as the set of strong ground motions used as inputs to adjacent buildings. The response quantities used to characterize damage of adjacent buildings are also stated in this section. The details of this information are provided in the following three subsections.

4.1. System parameters

The dynamic parameters of adjacent structures considered in this study are taken from an earlier study by Jankowski [10]. The mass, damping ratio and initial stiffness are taken as 7.5×10^4 kg, 0.05, 1.32×10^9 N/m for the left building and 3.0×10^6 kg, 0.05, 1.75×10^6 N/m for the right building. According to these parameters, one of the two buildings is flexible ($T_n = 1.2$ s) and lighter (left building) while the other building is stiffer ($T_n = 0.3$ s) and heavier (right building). Furthermore, the yield strength for the left and right buildings are taken as $f_{y_l} = 1.369 \times 10^5$ N, and $f_{y_r} = 1.442 \times 10^7$ N, respectively. The numerical values for the parameters of the nonlinear viscoelastic model for the pounding force are taken as $\bar{\beta} = 2.75 \times 10^9$ N/m^{3/2}, $\zeta = 0.35$ and $e = 0.65$ [10].

4.2. Input ground motion

A set of 3 horizontal ground motion records with different peak ground accelerations (PGA) are used as input to adjacent buildings. These records are the first horizontal component of the 1989 Loma Prieta recorded at SF Intern. Airport with 0.24g PGA and site-source of 64.4 km, the 90° horizontal component of the 1999 Kocaeli recorded at Sakarya recording station with 0.37g PGA and site-source of 3.1 km and the first horizontal component of the 1995 Kobe earthquake recorded at KJMA with 0.82g PGA and site-source of 0.60 km. These records represent strong ground motion records with different frequency content, total duration, site-source distance and local soil conditions.

4.2. System responses

In this paper, the response of adjacent buildings is assessed in terms of the maximum ductility demand, the pounding force f_1 , input and dissipated energies and damage indices of Eqns (2.1-2.4). The input energy to the structure by the earthquake and the associated damping, hysteretic, elastic and kinetic energies dissipated by the structure can be estimated from the energy balance of the equation of motion for the structure (see Eqn. 3.1) as [21-23]:

$$\int_0^t m_1 \ddot{u}_1(\tau) \dot{u}_1(\tau) d\tau + \int_0^t c_1 \dot{u}_1^2(\tau) d\tau + \int_0^t r_1(\tau) \dot{u}_1(\tau) d\tau + \int_0^t f_1(\tau) \dot{u}_1(\tau) d\tau = - \int_0^t m_1 \ddot{u}_g(\tau) \dot{u}_1(\tau) d\tau \quad (4.1)$$
$$E_K(t) + E_D(t) + E_S(t) + E_P(t) = E_I(t)$$

Eqn. 4.1 represents the relative energy terms for the left building. Here $E_I(t)$ is the earthquake relative input energy to the structure since ground starts shaking until it comes to rest. $E_K(t)$ is the relative kinetic energy ($E_K(t) = m_1 \dot{u}_1^2(t)/2$) and $E_D(t)$ is the energy absorbed by damping. The energy $E_S(t)$ represents the total relative energy absorbed by the spring and is composed of the recoverable elastic energy and the hysteretic cumulative plastic energy $E_H(t)$. $E_P(t)$ is the energy arising due to pounding force between the two buildings. Similar energy terms for the right building can be determined from the equation of motion following the same procedures for the right building.

5. NUMERICAL RESULTS AND DISCUSSION

This section provides numerical illustrations of the formulation developed in this paper for fixed-base

adjacent insufficiently separated buildings. In the numerical analysis, the acceleration records have been scaled to 0.50 g PGA to ensure inelastic response of structures and the separation distance d is taken equal to 0.05 m. The separation distance is changed later to examine its effect on the response of adjacent buildings. The parameters of the damage indices are taken as $\mu_{u_l} = \mu_{u_r} = 6.0$, and $\gamma = 0.15$.

The structural response of both buildings is calculated using Newmark- β method in the Matlab platform ($\alpha = 0.25$, $\beta = 0.50$ and $\Delta t = 0.005$ s).

The numerical results for adjacent buildings are presented in Figs. 5.1.-5.5. Fig. 5.1. shows the response quantities for left and right buildings under Loma Prieta earthquake record. Specifically, this figure depicts the displacement, pounding force and damage indices in time domain for both buildings. Note that pounding occurs between the two buildings twice for a very short time duration which is seen in the displacement plot where displacements of left and right buildings intersect. The plot of the pounding force implies also that pounding starts at the same time instant and lasts for a very short duration of time. Notice that the pounding force is the same quantity for both buildings. However, its effect on each building may be different (recall that the left building is flexible while the right building is rigid and that the two buildings have different responses under the same earthquake). With this in mind, we show the hysteretic loops (hysteretic force versus displacement) and the pounding loops (pounding force versus displacement) for both buildings under the 1999 Kocaeli ground acceleration in Fig. 5.2. The figure reflects the fact that the building on right has more hysteretic loops and more

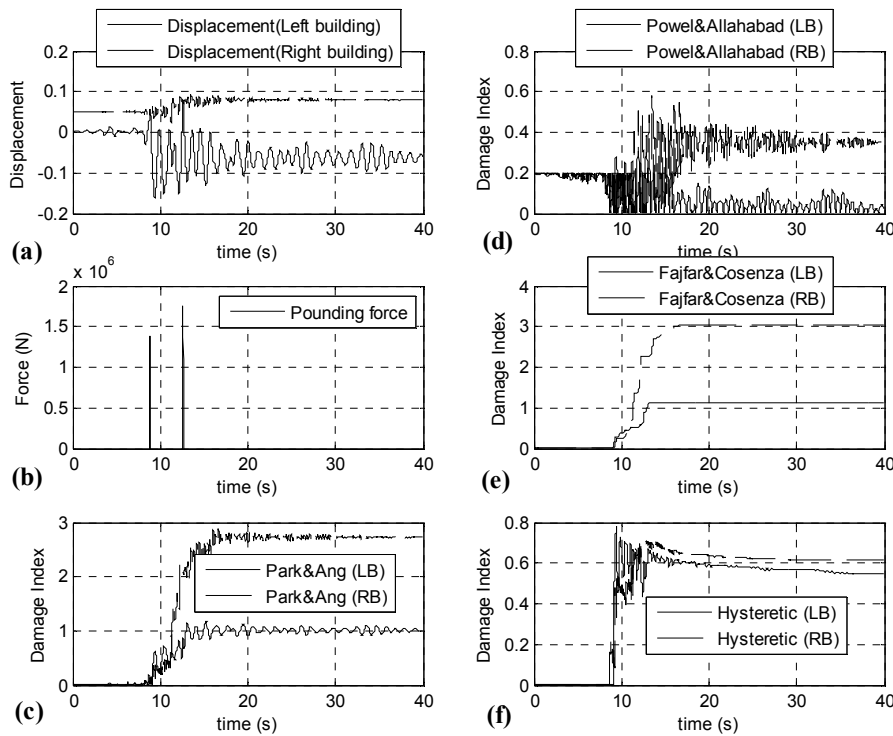


Figure 5.1. Response parameters for fixed-base buildings to Loma Prieta record (a) Displacements (b) Pounding force (c) Park and Ang damage index (d) Powell and Allahabadi damage index (e) Fajfar and Cosenza damage index (f) Damage index based on hysteretic energy

dissipated hysteretic energy compared to the building on left. It can be noticed also that the pounding loops for the building on right is wider compared to that on left. This observation is supported by the higher values of ductility factor and damage index for the building on right compared to the same quantities for the building on left. For instant, $\mu = 1.99$, $DI_{PA} = 0.54$, $DI_{AP} = 0.20$, $DI_{FC} = 0.27$, $DI_H = 0.41$ for the left building while $\mu = 2.35$, $DI_{PA} = 0.97$, $DI_{AP} = 0.27$, $DI_{FC} = 0.89$, $DI_H = 0.63$ for right

building. Note that, according to Park and Ang damage criterion, the left building experiences unreparable damage while the right building is fully collapsed. In fact, the obtained numerical values of energies reflect that the hysteretic energy is substantially higher than the pounding energy which can be expected given that pounding occurs for short durations (note that for a sufficiently large separation distance pounding may not occur leading to zero pounding force and zero pounding energy). The same fact is also reflected in the input and dissipated energies for both buildings where those for left building are $E_I = 25.06 \text{ kN m}$, $E_D = 20.46 \text{ kN m}$ and $E_H = 12.17 \text{ kN m}$ while those for the right building are $E_I = 1474.60 \text{ kN m}$, $E_D = 857.67 \text{ kN m}$ and $E_H = 703.52 \text{ kN m}$.

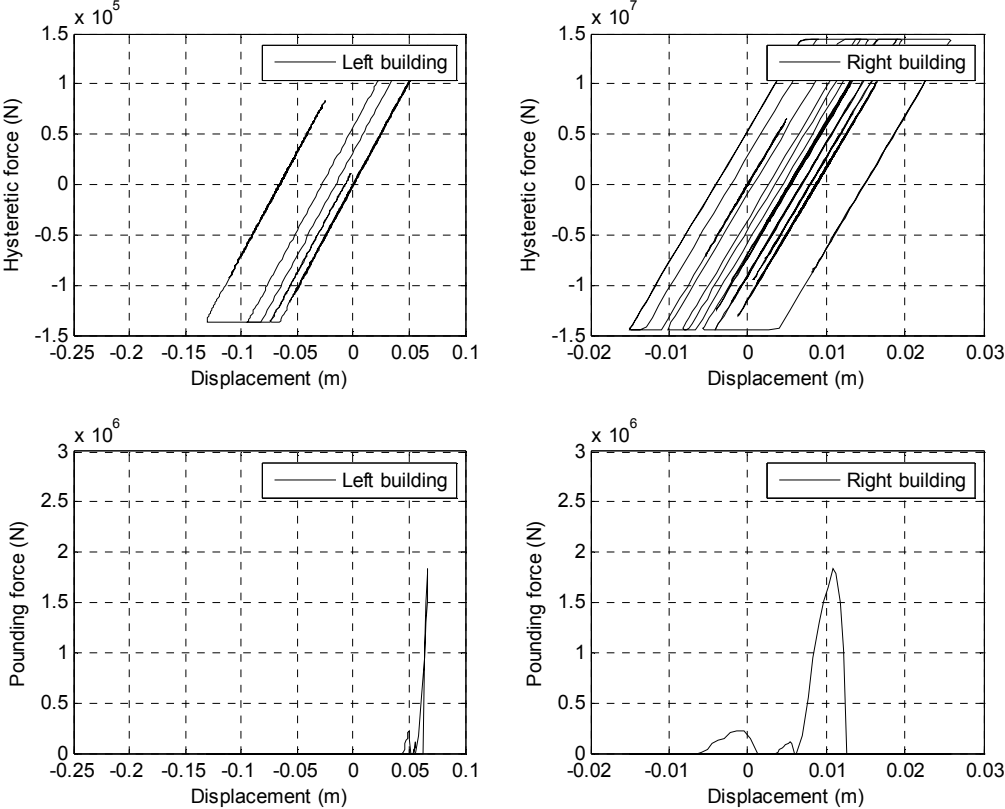


Figure 5.2. Hysteretic and pounding forces for adjacent buildings under Kocaeli record

Fig. 5.3. and Fig. 5.4 show the input energy and dissipated (yielding, damping and kinetic) energy for the fixed-base adjacent buildings under the Loma Prieta earthquake record (far-fault) and the Kobe earthquake record (near-fault), respectively. For the given structures and separation distance, it has been observed that near-fault earthquakes exert less input energy on adjacent structures than far-fault earthquakes. Consequently, adjacent buildings dissipate less energy under near-fault earthquakes compared with far fault earthquakes. In both cases, however, the input energy to both structures is dissipated mainly by yielding and damping mechanisms. The strain and kinetic energies are very small compared to the yield and damping energies. The kinetic energy reaches its maximum value during the strong phase of the ground acceleration and diminishes by the end of the ground shaking. To examine the effect of the separation distance on peak response quantities of adjacent buildings, the value of the gap distance between adjacent buildings (d) is varied between 0 and 0.20 m and the peak response of both buildings is determined for each separation distance. Fig. 5.5. shows the peak damage indices for both buildings under the 1995 Kobe earthquake. It is seen that the separation distance has substantial influence on the peak response of both buildings. For example, the peak damage indices increase when the separation distance decreases. Pounding does not occur between adjacent buildings for a separation distance of about 0.10 m where the damage indices for adjacent buildings stabilize and approach

constant values. This implies that the damage index for both buildings does not include contribution from pounding since the pounding force vanishes and pounding effects diminish.

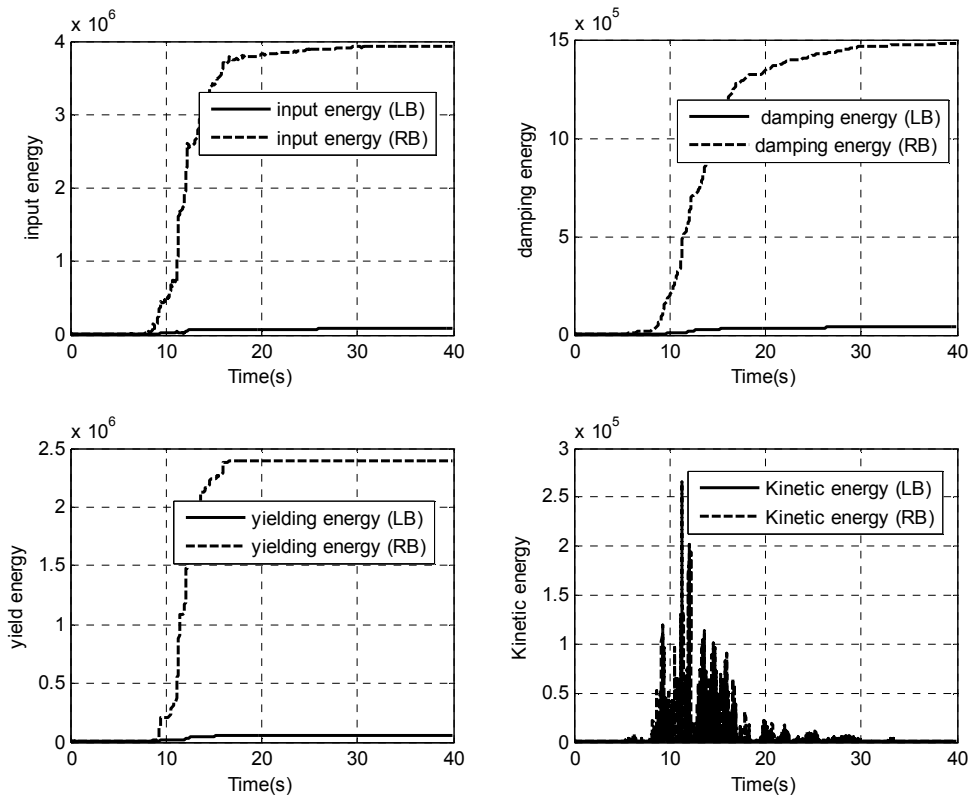


Figure 5.3. Input and dissipated energy for adjacent buildings under Loma Prieta earthquake (far fault)

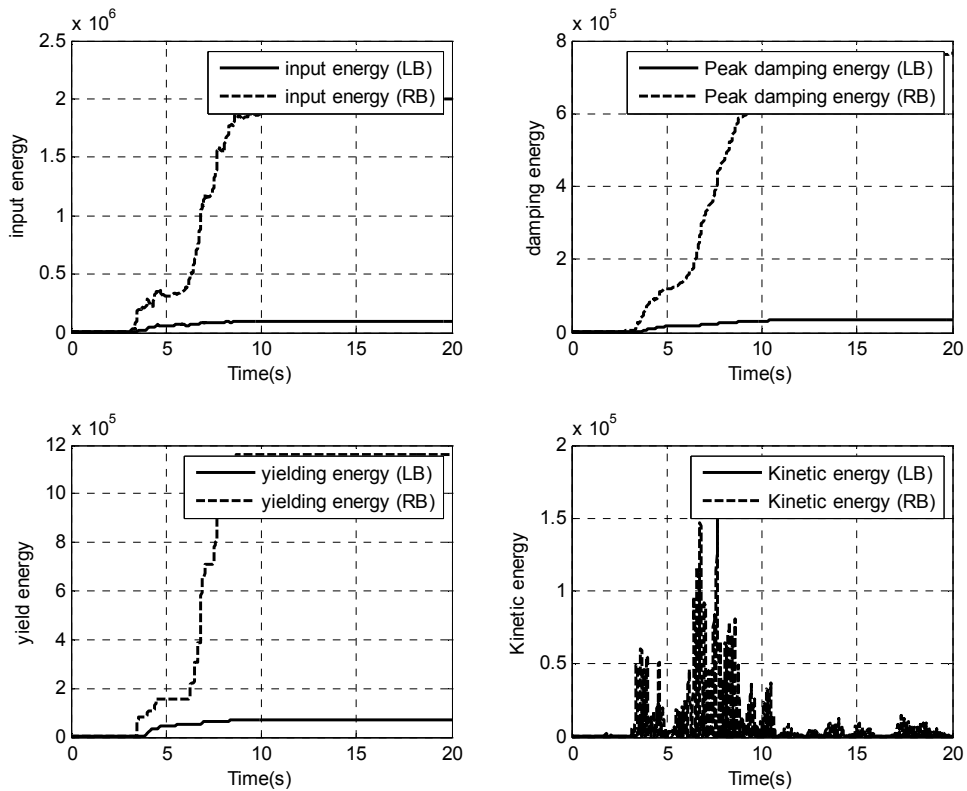


Figure 5.4. Input and dissipated energy for adjacent buildings under Kobe earthquake (near fault)

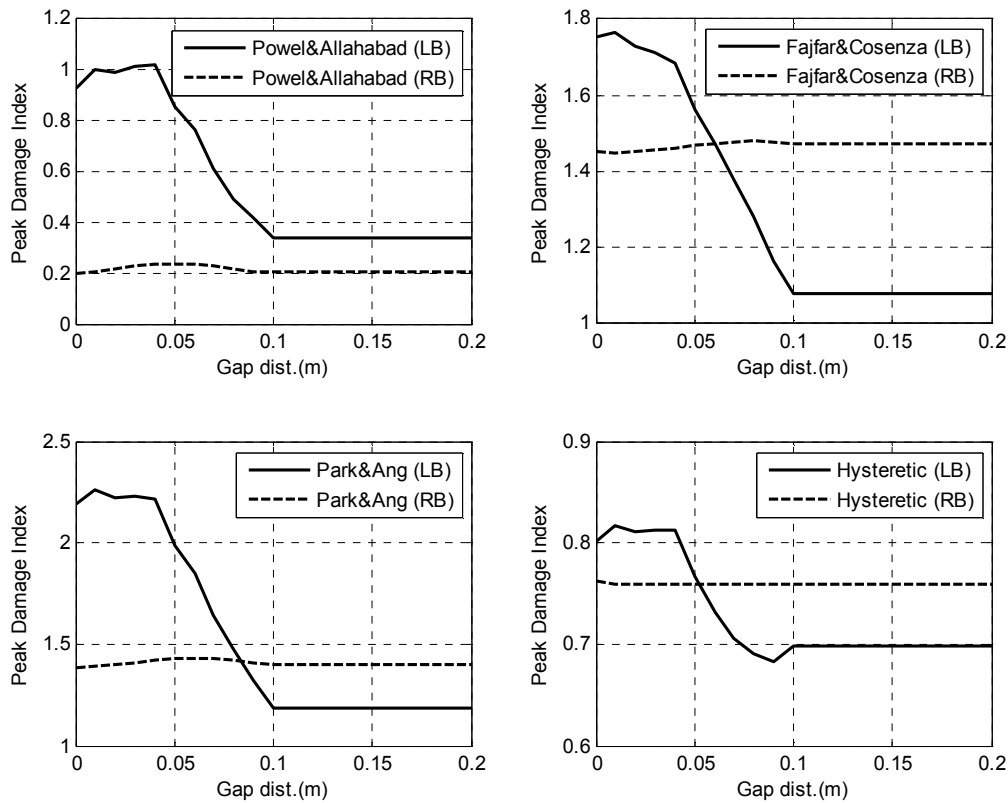


Figure 5.5. Influence of separation distance between adjacent buildings on damage indices under Kobe earthquake

6. CONCLUSIONS

This paper tackles damage assessment of adjacent buildings with fixed bases under earthquake loads. Earlier studies on response analysis of adjacent buildings under earthquake loads have focused on pounding effect in terms of the displacement, velocity and acceleration and associated pounding force. This study explores the ductility, pounding force, input energy and dissipated energy by damping and yielding and damage indices in neighboring buildings caused by earthquake loads. Damage indices include those developed by Park and Ang, Fajfar and Cosenza, Allahabadi and Powell and the damage index estimated based on hysteretic energy dissipated by yielding. These response parameters are believed to be of significant importance in assessing damage of adjacent buildings since they provide a quantitative measure of damage level and, hence, a decision on necessary repair can be taken. For instant, the inelastic response of both structures may not provide an efficient measure of the structural performance compared to damage indices which provide a quantitative measure of the structural performance. Additionally, this study has investigated the influence of the separation distance between adjacent buildings on the associated structural response and damage indices. It has been concluded that damage indices increase as the separation distance decreases due to the effect resulting from the pounding force between adjacent buildings.

In the present study, pounding of simple structures of equal height modeled as SDOF systems with elastic-plastic force-deformation relationship is studied. Future research work will focus on investigating damage of adjacent MDOF structures of different heights with degrading nonlinear models, accounting for formation of plastic hinges. In this case, a weighted summation of local damage indices of individual structural members can be used as an estimate of the global damage index for the structure. Additionally, examining the damage of adjacent buildings under probabilistic

ground motion inputs is also of significant interest to structural engineers and will be considered in a future study.

ACKNOWLEDGEMENT

This research is funded by the Deanship of Scientific Research (DSR), King Abdulaziz University, Jeddah, under grant No. 9-829-D1432. The authors acknowledge with thanks DSR technical and financial support.

REFERENCES

- [1] Moustafa, A. (2012). *Earthquake-resistant structures: Design, assessment and rehabilitation*, Intech, Croatia.
- [2] Rosenbluth, E. and Meli, R. (1986). The 1985 earthquake: causes and effects in Mexico City. *Concrete International (ACI)* **8**: 23–36.
- [3] Anagnostopoulos, S.A. (1988). Pounding of buildings in series during earthquakes. *Earthquake Engineering & Structural Dynamics* **16**:3, 443–456.
- [4] Jankowski, R., Wilde, K. and Fujino, Y. (1998). Pounding of superstructure segments in isolated elevated bridge during earthquakes. *Earthquake Engineering & Structural Dynamics* **27**:5, 487–502.
- [5] Mahmoud, S. and Jankowski, R. (2010). Pounding-involved response of isolated and non-isolated buildings under earthquake excitation. *Earthquake and Structures* **1**:3, 3250–3262.
- [6] Athanassiadou, C.J. and Penelis, G.G. (1985). Elastic and inelastic system interaction under an earthquake motion. *Proceedings of the 7th Hellenic Conference on Concrete*, Patras, Greece, 211–216
- [7] Pantelides C.P. and Ma, X. (1998). Linear and nonlinear pounding of structural systems. *Computer and Structures* **66**:1, 79–92, 1998
- [8] Muthukumar, S. And DesRoches, R. (2006). A Hertz contact model with nonlinear damping for pounding simulation. *Earthquake Engineering & Structural Dynamics* **35**:7, 811–828.
- [9] Jankowski, R. (2006). Pounding force response spectrum under earthquake excitation. *Engineering Structures* **28**:8, 1149–1161.
- [10] Jankowski, R. (2008). Earthquake-induced pounding between equal height buildings with substantially different dynamic properties. *Engineering Structures* **30**:10, 2818–2829.
- [11] Moustafa, A. (2011). Damage-based design earthquake loads for single-degree-of-freedom inelastic structures. *Journal of Structural Engineering (ASCE)* **137**:3, 456–467.
- [12] Fajfar, P. (1992). Equivalent ductility factors, taking into account low-cyclic fatigue, *Earthquake Engineering & Structural Dynamics*, **21**:10, 837–848.
- [13] Cosenza, C., Manfredi, G. and Ramasco, R. (1993). The use of damage functionals in earthquake engineering: a comparison between different methods, *Earthquake Engineering & Structural Dynamics* **22**:10, 855–868.
- [14] Powell, G.H. and Allahabadi, R. (1988). Seismic damage predictions by deterministic methods: concepts and procedures, *Earthquake Engineering & Structural Dynamics*, **16**:5, 719–734.
- [15] Park, Y.J. and Ang, A.H.S. (1985). Mechanistic seismic damage model for reinforced concrete, *Journal of Structural Engineering*, ASCE **111**:4, 722–739.
- [16] Park, Y.J., Ang, A.H.S. and Wen, Y.K. (1985). Seismic damage analysis of reinforced concrete buildings, *Journal of Structural Engineering*, ASCE, **111**:4, 740–757.
- [17] Park, Y.J., Ang, A.H.S. and Wen, Y.K. (1987). Damage-limiting aseismic design of buildings, *Earthquake Spectra* **3**:1, 1–26.
- [18] Chopra, A.K. (2006), *Dynamics of Structures*. 3rd edition, Prentice Hall; New York.
- [19] Jankowski, R. (2005). Non-linear viscoelastic modelling of earthquake-induced structural pounding. *Earthquake Engineering & Structural Dynamics* **34**:6 595–611.
- [20] Jankowski, R. (2006). Analytical Expression Between the Impact Damping Ratio and the Coefficient of Restitution in the Nonlinear Viscoelastic Model of Structural Pounding,” *Earthquake Engineering & Structural Dynamics*, **35**:4, 517–524.
- [21] Zahrah, T.F. and Hall, W.J. (1984). Earthquake energy absorption in sdof structures. *Journal of Structural Engineering* **110**:8, 1757–1772.
- [22] Uang, C.M and Bertero, V.V. (1990). Evaluation of seismic energy in structures. *Earthquake Engineering & Structural Dynamics* **19**:1, 77–90.
- [23] Abbas, A.M. (2006). Critical earthquake load inputs for simple inelastic structures. *Journal of Sound and Vibration* **296**:4–5, 949–967.